

## CHAPTER 321

# Wave Overwash of Subaerial Dunes

Yukiko Tega <sup>1</sup> and Nobuhisa Kobayashi, M. ASCE <sup>2</sup>

### Abstract

Small-scale experimental results consisting of 72 runs for minor to major dune overwash are analyzed to improve existing dune erosion models that do not account for wave overwash processes explicitly. The measured cross-shore sediment transport rate is found to vary approximately linearly from the measured rate somewhat below the still water level, which is affected by the overwash intensity, to the overwash rate over the dune crest. The measured overwash sand concentration for the sand with its median diameter of 0.38 mm used in this experiment was in the range of 0.02 to 0.06. The time-dependent one-dimensional numerical model for the overtopping flow combined with two sediment transport formulas indicates that the overwash sand concentration may be on the order of 0.04 except for very fine or coarse sands.

### Introduction

The quantitative understanding of wave overwash of dunes is essential for predicting dune erosion as well as coastal flooding hazards during storms. Existing dune erosion models generally assume that the net sediment transport rate may be extrapolated linearly from the value slightly below the still water level (SWL) to zero at the upper limit of wave runup estimated empirically. This linear extrapolation may be necessary for lack of a simple swash model and appears to be a reasonable first approximation for the case of no overwash.

A simple empirical method for predicting the onshore sand transport rate associated with wave overwash of subaerial dunes is presented herein by expanding the experimental study by Hancock and Kobayashi (1994). The experiment was limited to subaerial dunes, while experiments on submerged dunes were conducted by Steetzel and Visser (1992). Kobayashi et al. (1996) showed that the measured reflection coefficient and overtopping rates could be predicted using the empirical formulas developed for coastal structures and adjusted for dunes. This paper examines the cross-shore sand transport on dunes.

### Experiment

Fig.1 shows the setup of the dune overwash experiment conducted in a wave tank that was 30 m long, 2.44 m wide, and 1.5 m high. The experiment was

---

<sup>1</sup>Technical Research Institute, Nishimatsu Construction Co.Ltd., 2570-4 Shimotsuruma, Yamato, Kanagawa, 242, Japan

<sup>2</sup>Professor and Associate Director, Center for Applied Coastal Research, University of Delaware, Newark, DE 19716.

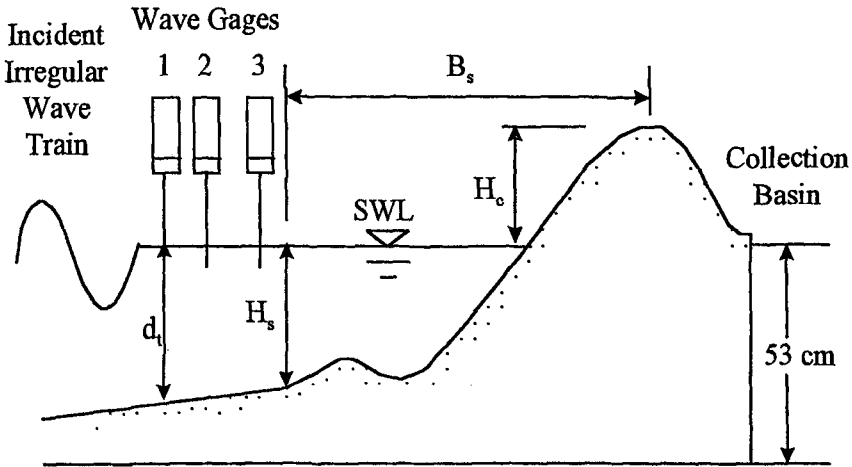


Figure 1: Experimental Setup.

conducted in a 61 cm wide channel by constructing a divider wall to reduce the effects of re-reflection from the wave paddle used to generate irregular waves. The well-sorted sand with a median diameter of 0.38 mm was placed in front of a 53 cm high basin used to collect both overtopped water and overwashed sand. The measured specific gravity, porosity and fall velocity of the sand were 2.66, 0.41 and 5.29 cm/s, respectively. Three wave gages placed immediately seaward of the breaker zone were used to separate the incident and reflected waves at wave gage 1 for each run (Kobayashi and Raichle 1994). The duration of each run was 325 s and the sampling rate for the three gages was 20 Hz.

Seven tests, referred to as tests A to G hereafter, were conducted for minor to major overwash. The dune crest was initially located at approximately 12 cm above SWL and at a horizontal distance of 40 cm from the basin wall. Each test consisted of a series of runs to examine the changes of the overtopping rate per unit width,  $Q$ , and the overwash rate per unit width,  $Q_s$ , as the beach and dune profile evolved. The overtopping and overwash rates per unit width,  $Q$  and  $Q_s$ , for each run were obtained by dividing the volumes of water and sand, respectively, collected in the basin by the run duration 325 s and the channel width 61 cm. The value of  $Q_s$  is based on the sediment volume only without any void. The test was terminated just before the collection basin wall would become exposed to direct wave action. Beach and dune profiles were measured along three lines using an ultrasound profiler at the beginning and end of each test and after runs of noticeable profile changes. The average profile of the measured three profiles was used to find the dune crest height  $H_c$  above SWL, the location where the depth below SWL equals to the significant wave height  $H_s$  measured at wave gage 1, and the horizontal distance  $B_s$  from the dune crest to this location as shown in Fig. 1. The equivalent uniform slope for wave overtopping,  $m_o$ , is assumed to be given by  $m_o = (H_c + H_s)/B_s$ . The measured values of  $m_o$  were interpolated to obtain the value of  $m_o$  in the middle of each run.

Table 1 lists the number of runs in each test and the ranges of the incident wave characteristics at wave gage 1, the dune crest height  $H_c$ , the equivalent slope  $m_o$ , the overtopping rate  $Q$  and the overwash rate  $Q_s$  for the seven tests. The water depth  $d_t$  below SWL at wave gage 1 for each test was constant where the bottom change at wave gage 1 was negligible. The spectral peak period  $T_p$  was

Table 1: Ranges of Incident Wave Characteristics, Dune Crest Height, Overtopping, Overwash Rates and Equivalent Slope for 7 Tests

Test	Number of runs	$d_t$ (cm)	$T_p$ (s)	$H_s$ (cm)	$H_c$ (cm)	$Q$ ( $\text{cm}^2/\text{s}$ )	$Q_e$ ( $\text{cm}^2/\text{s}$ )	$m_o$
A	10	44.3	1.2	11.8-12.2	7.5-12.2	0-0.40	0-0.0148	0.11-0.26
B	9	43.4	1.4	12.2-12.5	7.1-11.1	0.52-1.08	0.024-0.040	0.11-0.25
C	8	44.8	1.6	12.3-12.8	7.0-10.9	1.51-2.61	0.059-0.089	0.11-0.25
D	7	43.7	1.8	12.1-12.4	7.6-11.0	3.33-4.68	0.12-0.16	0.14-0.24
E	5	43.2	2.0	12.4-12.7	6.7-10.7	6.33-8.72	0.30-0.37	0.16-0.25
F	24	43.2	1.4	12.0-12.3	7.9-11.3	0.31-0.47	0.007-0.026	0.09-0.16
G	9	43.2	2.0	12.0-12.4	7.8-11.1	2.89-4.38	0.10-0.16	0.11-0.16

also constant for each test and  $T_p = 1.2 - 2.0$  s for the seven tests. The significant wave height,  $H_s$ , based on a zero upcrossing method varied little during each test and among the seven tests because the TMA spectra with the spectral significant wave height  $H_{m0} = 12.5$  cm and  $T_p = 1.2 - 2.0$  s at the wave paddle were used to generate the incident irregular waves. On the other hand, the dune crest height  $H_c$  and the equivalent slopes  $m_o$  decreased with the increase of run number as the beach and the dune profile evolved. The data from tests A to E consisting of 39 runs were presented by Hancock and Kobayashi (1994). These tests corresponded to high dunes with large storm surge. Two additional tests, F and G, consisting of 33 runs were conducted by placing more sand in front of the initial dune profile used in tests A to E to reduce the water depth at the toe of the dune.

## Data Analyses

First, the measured overwash rate  $Q_o$  is related to the measured overtopping rate  $Q$  in the form

$$Q_o = C_s Q \quad (1)$$

where  $C_s$  is the average volumetric sediment concentration in the overwash. The dimensional values of  $Q_o$  and  $Q$  are plotted in Fig. 2 to show that these values were from the small scale experiment. Fig. 2 shows that the 72 data points fall within the narrow range of  $C_s = 0.02 - 0.06$  and that the empirical formula (1) with  $C_s \approx 0.04$  may be used to estimate  $Q_o$  for  $Q$  predicted separately. The subsequent sections will examine whether the assumption of constant  $C_s$  holds for field conditions and other sands.

To predict the overtopping rate  $Q$  for normally incident breaking waves on dunes, Kobayashi et al. (1996) adjusted the empirical formula for

wave overtopping on coastal structures proposed by Van der Meer and Janssen (1995). The toe of a coastal structure was assumed to correspond to the location of wave gage 1 immediately seaward of the breaker zone. The equivalent uniform slope  $m_o$  was assumed to represent the overall slope effect on wave overtopping of dunes. The adjusted formula was shown to yield the agreement between the measured and empirical values of  $Q$  almost within the 95 % confidence limits of the original formula based on about 500 data points. Fig. 3 shows the measured overwash rate  $Q_o$  as a function of the empirical overtopping rate  $Q_e$  based on the adjusted formula by Kobayashi et al. (1996). The formula (1) with  $Q$  replaced by  $Q_e$  is still reasonable. However, most of the values of  $C_s$  are in the range of  $C_s = 0.01 - 0.04$  with a typical value of  $C_s = 0.02$ . These values of  $C_s$  are smaller than those of  $C_s$  based on  $Q$  by a factor of about two. This is because the adjust formula for  $Q_e$  tends to overpredict the overtopping rates for the tests with larger

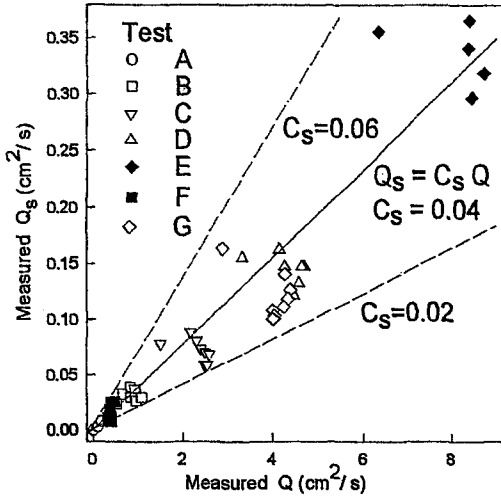


Figure 2: Measured Overwash Rate  $Q_s$  vs. Measured Overtopping Rate  $Q$ .

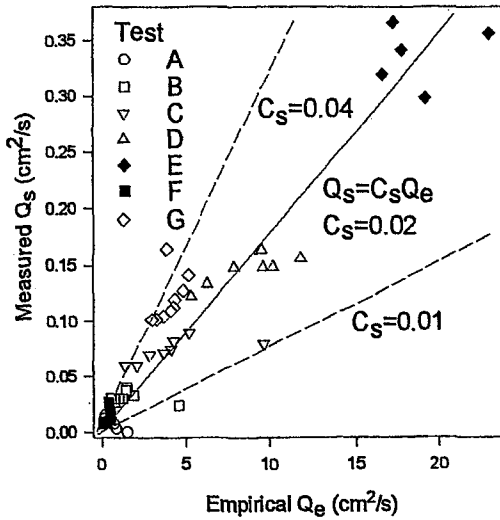


Figure 3: Measured Overwash Rate  $Q_s$  vs. Empirical Overtopping Rate  $Q_e$ .

overtopping rates. The accurate prediction of  $Q_s$  using (1) requires the accurate predictions of  $C_s$  and  $Q$ . Unfortunately, only the order of magnitude of  $Q$ , even for coastal structures, can be predicted at present. Consequently, the present study aims at the prediction of  $C_s$  within a factor of about two.

In order to predict the beach and dune profile evolution, the cross-shore variation of the net sediment transport rate is required. The net cross-shore sediment transport rate  $q_s$  was calculated using the continuity equation of sediment and the measured profiles starting from the seaward location of no profile change as described by Hancock and Kobayashi (1994). The value of  $q_s$  at the landward

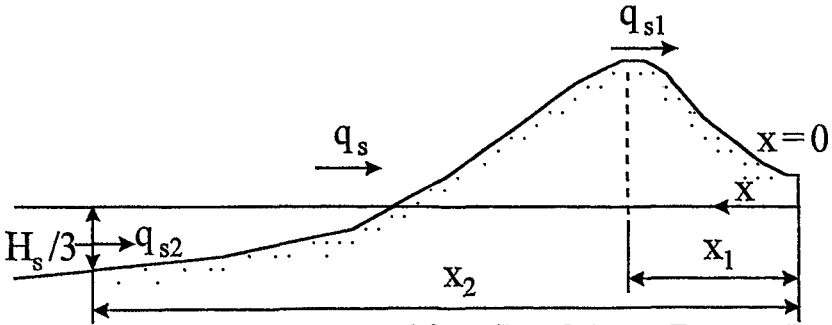


Figure 4: Schematic Representation of Cross-Shore Sediment Transport Rate  $q_s$  over Dune

boundary should correspond to the net sediment transport rate into the collection basin but was not exactly the same as the average overwash rate for the same duration calculated from the collected sand because of small profile measurement errors. As a result, the normalized results are presented as explained in the following.

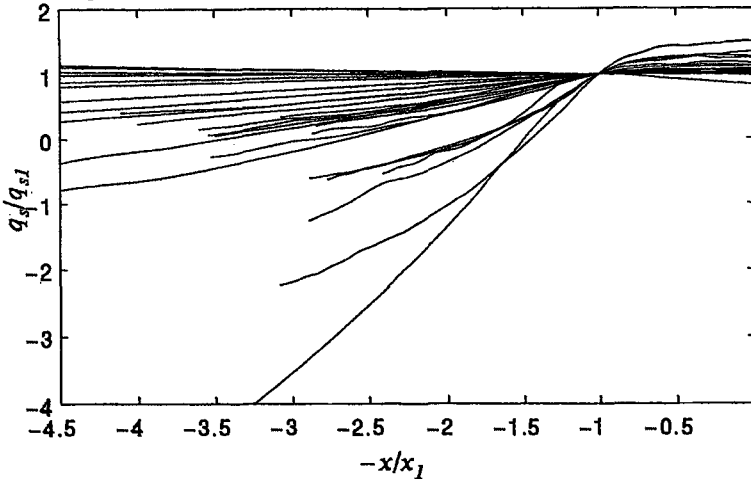


Figure 5: Normalized Cross-Shore Sediment Transport Rate,  $q_s/q_{s1}$ , as a Function of  $-x/x_1$  with  $x = 0$  at Edge of Collection Basin.

The measured cross-shore sediment transport rate  $q_s$  is taken to be positive onshore as shown in Fig. 4 where  $x =$  cross-shore coordinate taken to be positive seaward with  $x = 0$  at the edge of the collection basin. The dune crest is located at  $x = x_1$ . The seaward limit of this analysis may be taken at the location  $x_2$  where the water depth below SWL equals  $H_s/3$  because this depth of  $H_s/3$  is larger than the typical smallest depth adopted by existing cross-shore sediment transport models in the surf zone. The values of  $q_s$  at  $x = x_1$  and  $x_2$  are denoted by  $q_{s1}$  and  $q_{s2}$ , respectively. The locations of  $x_1$  and  $x_2$  varied somewhat between the two profiles measured consecutively. The first of the two profiles was used to find  $x_1$  and  $x_2$ . The average value of  $H_s$  during the runs between the two profile measurements was used for the depth  $H_s/3$  for  $x_2$ . The results presented in the

following are not sensitive to the details of the data analysis.

The normalized cross-shore sediment transport rate,  $q_s/q_{s1}$ , is plotted in Fig. 5 as a function of  $-x/x_1$  in the range  $0 < x < x_2$  for all the cross-shore variations of the onshore sand transport rate based on the consecutive profile measurements. Fig. 5 shows that the value of  $q_s$  landward of the dune crest is almost constant and may be approximated by the overwash rate  $Q_s$ , which is based on the sand volume collected in the basin for each run and should be more accurate than  $q_s$ . Furthermore,  $q_s$  increases approximately linearly from  $q_{s2}$  at  $x = x_2$  somewhat below SWL to  $q_{s1}$  at the dune crest. Consequently, the cross-shore variation of  $q_s$  required for the prediction of the dune profile evolution using the continuity equation for sediment may be represented by  $Q_s \simeq q_{s1}$  and  $q_{s2}$  where  $Q_s$  may be estimated using (1).

Existing dune erosion models estimate the cross-shore sediment transport rate slightly below SWL without regard to wave overwash. To examine the effect of overwash on  $q_s$  below SWL, the values of  $q_{s2}/q_{s1}$  are plotted as a function of the overtopping rate  $Q$  and the overwash rate  $Q_s$  in Fig. 6. Since  $q_{s1} > 0$  in this experiment, the positive and negative values of  $q_{s2}/q_{s1}$  imply the onshore and offshore sediment transport at  $x = x_2$  below SWL, respectively. Fig. 6 indicates that the net sediment transport somewhat below SWL in this experiment was offshore for small  $Q$  and  $Q_s$  but tended to become onshore with the increase of  $Q$  and  $Q_s$ . This implies that the estimation of  $q_{s2}$  will need to account for wave overtopping and overwash.

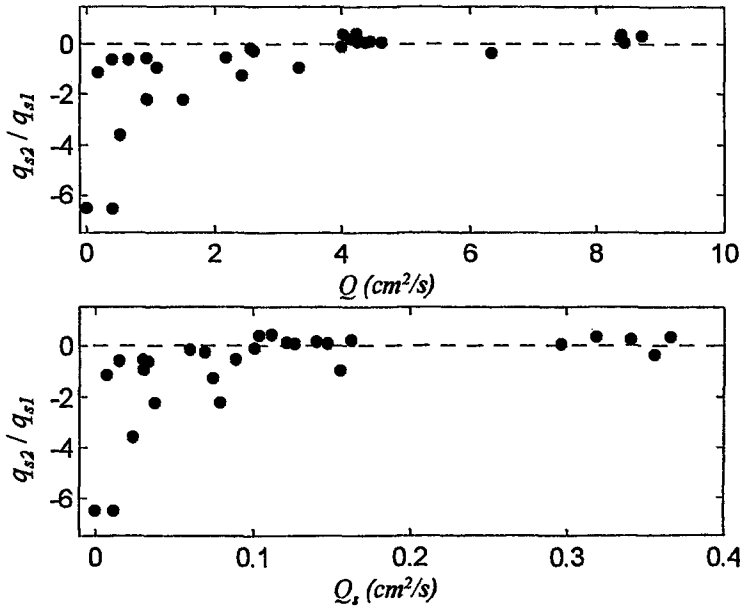


Figure 6: Normalized Sediment Transport Rate  $q_{s2}/q_{s1}$ , Somewhat below SWL as a Function of Overtopping Rate  $Q$  (top) and Overwash Rate  $Q_s$  (bottom)

## Numerical Modeling

To elucidate the overwash processes and extrapolate the small-scale experimental results presented above, use is made of the time-dependent one-dimensional numerical model RBREAK2 (Kobayashi and Poff 1994). RBREAK2 was shown

to predict the overtopping rates for revetments in surf zones within about 40 % errors (Kobayashi and Raichle 1994). Two sediment transport formulas are combined with RBREAK2 to predict the net sediment transport rate  $q_s$ .

The empirical formula proposed by Trowbridge and Young (1989) for unbroken water waves under sheet flow conditions may be used to express  $q_s$  in the form

$$\frac{q_s}{wd} = \frac{A\overline{|u|u}}{g(s-1)d} \quad (2)$$

in which  $w$  = fall velocity of the sand particle;  $g$  = gravitational acceleration;  $d$  = median diameter  $d_{50}$  where  $d$  is used for brevity;  $s$  = specific gravity of the sand;  $u$  = instantaneous depth-averaged velocity computed by RBREAK2 ; and  $A$  = empirical parameter. The overbar in (2) denotes the time-averaging for the duration of each run. The formula (2) with  $A \simeq 0.25$  was employed successfully to predict the onshore sand transport outside the surf zone at the CERC Field Research Facility.

On the other hand, Ribberink and Al-Salem (1994) developed a sediment transport formula using large oscillating water tunnel data. This formula expresses  $q_s$  as

$$\frac{q_s}{wd} = af^{1.5} \frac{\overline{u^3}}{w^3} \quad (3)$$

where  $a$  = empirical parameter; and  $f$  = Jonsson's wave friction factor. The formula with  $a = \sqrt{2}$  was shown to yield good agreement with their water tunnel data.

Table 2: Measured and Computed Overtopping Rates for 10 Runs

Test	$f$	$T_p$ (s)	$H_s$ (cm) (cm)	Measured $Q$ ( $cm^2/s$ )	Computed $Q_c$ ( $cm^2/s$ )
B6	0.014	1.4	12.36	0.93	0.38
B9	0.014	1.4	12.28	1.08	1.09
B9	0.012	1.4	12.28	1.08	1.06
B9	0.010	1.4	12.28	1.08	0.90
D5	0.012	1.8	12.30	4.63	1.98
D5	0.010	1.8	12.30	4.63	2.19
D7	0.012	1.8	12.29	4.46	1.78
D7	0.010	1.8	12.29	4.46	1.97
E1	0.010	2.0	12.49	6.33	2.16
E2	0.010	2.0	12.67	8.40	3.12
E3	0.010	2.0	12.71	8.38	13.07
G1	0.010	2.0	12.42	2.89	0.12
G2	0.010	2.0	12.34	4.26	0.23
G3	0.010	2.0	12.05	4.38	1.48

The formulas (2) and (3) developed for the sand transport due to prototype large-scale unbroken waves may be applied to the sand transport due to broken waves overtopping on dunes if the empirical parameters  $A$  and  $a$  are adjusted.

Computations were made for 10 representative runs using the measured profile and incident wave train at wave gage1 as input to RBREAK2 . Table 2 summarizes the computed runs where  $f$  = friction factor specified in the computation;

$T_p$  = spectral peak period of the incident waves;  $H_s$  = incident significant wave height;  $Q$  = measured overtopping rate; and  $Q_c$  = computed overtopping rate which is the time-averaged volume flux per unit width at the edge of the collection basin during each run. The friction factor  $f$  for the overtopping flow is expected to be different from Jonsson's friction factor. The value of  $f \approx 0.01$  is a reasonable estimate from the previous calibration for wave overtopping of revetments performed by Kobayashi and Raichle (1994). RBREAK2 with  $f = 0.01 - 0.014$  predicts the order of magnitude of the overtopping rates. For tests E and G, where the overall beach and dune slope was gentler for test G as may be inferred from the range of  $m_o$  listed in Table 1, the computed overtopping rates were varied much more than the measured rates for the different profiles of tests E and G and as the profile evolved in each test. This apparent sensitivity of RBREAK2 to the beach and dune profile is not certain for lack of measurements on the depth and velocity of the overtopping flow in this experiment.

The cross-shore variation of the net sediment transport rate  $q_s$  is also computed using (2) and (3) where RBREAK2 predicts the temporal and cross-shore variations of the depth-averaged velocity  $u$  during each run. The computed cross-shore variation of  $q_s$  in the region between the dune crest and the edge of the collection basin is essentially constant and consistent with the measured variation shown in Fig. 5. However, the computed values of  $q_s$  seaward of the dune crest vary too rapidly in comparison to these shown in Fig. 5. The assumption of the instantaneous response of sand particles to the depth-averaged velocity  $u$  made in (2) and (3) may not be valid seaward of the dune crest. The following analysis is limited to the computed results at the edge of the collection basin which are representative of the computed results landward of the dune crest.

The computed time series of the normalized water depth,  $h_* = h/H_s$ , where  $H_s$  = incident significant wave height for each run, and the normalized depth-averaged velocity,  $u_* = u/\sqrt{gH_s}$ , are stored at the sampling rate of 20 Hz during each run lasting 325 s. In order to find a relationship between  $h_*$  and  $u_*$ , the stored values of  $h_*$  and  $u_*$  for the 10 runs listed in Table 2 are plotted in the form

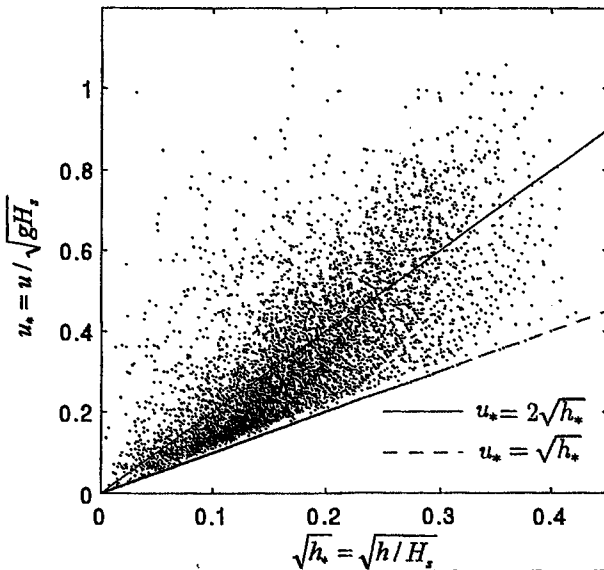


Figure 7: Computed Normalized Velocity,  $u_*$ , and Square Root Depth,  $h_*$ , of Overwash Flow for 10 Runs

of  $u_*$  v.s.  $\sqrt{h_*}$  in Fig. 7. RBREAK2 assumes that the overtopping flow at the landward boundary of the computation domain is critical ( $u = \sqrt{gh}$  and hence  $u_* = \sqrt{h_*}$ ) or supercritical ( $u > \sqrt{gh}$  and hence  $u_* > \sqrt{h_*}$ ). The scattered points in Fig. 7 may be represented crudely by the simple relationship,  $u_* \simeq 2\sqrt{h_*}$ . This relationship corresponds to that between the bore speed and flow depth on a barrier island measuring using video techniques by Holland et al. (1991) if the celerity and fluid velocity of the bore are assumed to be the same.

The simple relationship of  $u_* = 2\sqrt{h_*}$  may describe the overall trend of the overtopping flow but is not accurate enough to predict the instantaneous relationship between  $u_*$  and  $h_*$ . As an example, Fig. 8 shows the computed time series of  $u_*$  and  $2\sqrt{h_*}$  for run B9 where  $t_* = t/T_p$  is the normalized time with  $t_* = 0$  at the beginning of each run. The relationship of  $u_* = 2\sqrt{h_*}$  tends to underpredict the peaks of  $u_*$  and overpredict the receding segments of  $u_*$ .

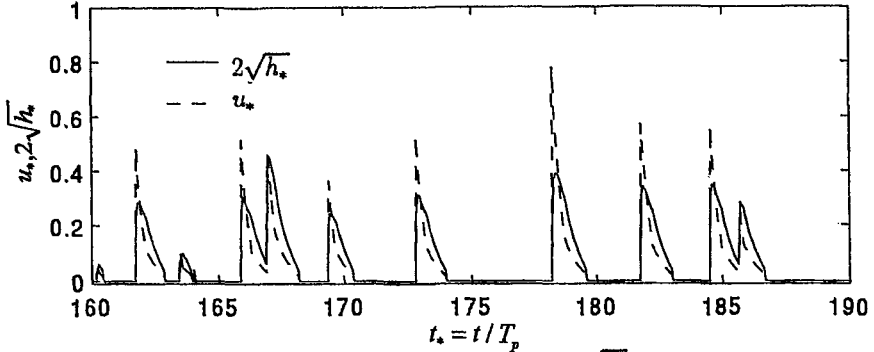


Figure 8: Computed Time Series of  $u_*$  and  $2\sqrt{h_*}$  for Run B9

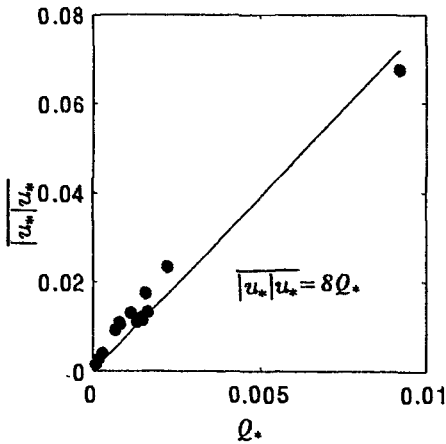


Figure 9: Computed Normalized Velocity Moment  $|u_*|u_*$  as a Function of Computed Normalized Overtopping Rate  $Q_*$ .

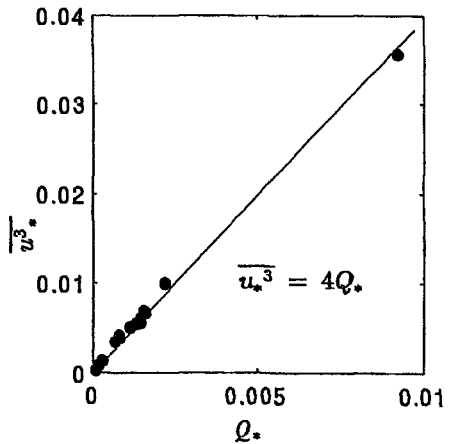


Figure 10: Computed Normalized Velocity Moment  $u_*^3$  as a Function of Computed Normalized Overtopping Rate  $Q_*$ .

In order to explain the approximate linear relationship between  $Q_s$  and  $Q$  expressed by (1) using the formulas (2) and (3), the computed time-averaged values of  $\overline{|u_*|u_*}$  and  $\overline{u_*^3}$  for each of the runs listed in Table 2 are plotted as a function of the computed normalized overtopping rate,  $Q_* = \overline{h_*}u_*$ , in Figs. 9 and 10, respectively. The dimensional overtopping rate  $Q$  is given by  $Q = H_s\sqrt{gH_s}Q_*$ . In Fig. 9,  $\overline{|u_*|u_*}/Q_* = 7.3 - 18.8$  and the linear regression coefficient is about 8.

In Fig. 10,  $\overline{u_*^3}/Q_* = 3.8 - 5.3$  and the relationship of  $\overline{u_*^3} = 4Q_*$  based on the assumption of  $u_* = 2\sqrt{h_*}$  yields very good agreement. These relationships together with (2) and (3) are used to express the overwash sand concentration  $C_s$  in (1) in terms of the sand and wave characteristics.

**Overwash Sand Concentration**

The overwash rate  $Q_s$  is estimated as the values of  $q_s$  in (2) and (3) at the edge of the collection basin. Substitution of (1) into (2) and (3) yields the following expressions of  $C_s$ :

$$C_s = Av_* \frac{\overline{|u_*|u_*}}{Q_*} \quad ; \quad w_* = \frac{w}{(s-1)\sqrt{gH_s}} \tag{4}$$

and

$$C_s = af^{1.5}d_* \frac{\overline{u_*^3}}{Q_*} \quad ; \quad d_* = \frac{gd}{w^2} \tag{5}$$

where  $w_*$  and  $d_*$  are the normalized fall velocity and diameter respectively. To calibrate the empirical coefficients  $A$  and  $a$  in (4) and (5), the measured concentration  $C_s$  is plotted as a function of  $w_*\overline{|u_*|u_*}/Q_*$  and  $f^{1.5}d_*\overline{u_*^3}/Q_*$  in Figs. 11 and 12, respectively, for the computed runs listed in Table 2. Fig. 11 indicates  $A \approx 0.1$  in (4) instead of  $A \approx 0.25$  calibrated by Trowbridge and Young (1989).

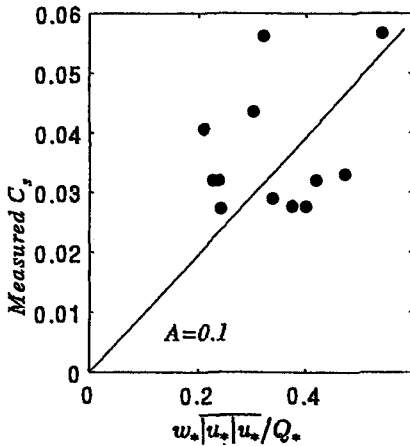


Figure 11: Measured Sand Concentration  $C_s$  Compared with Formula (4) with  $A = 0.1$

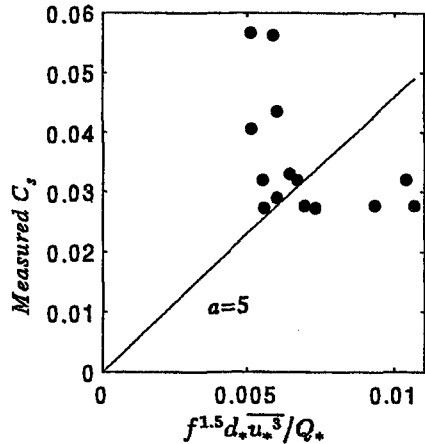


Figure 12: Measured Sand Concentration  $C_s$  Compared with Formula (5) with  $a = 5$

Fig. 12 suggests  $a \approx 5$  instead of  $a \approx \sqrt{2}$  obtained by Ribberink and Al-Salem (1994). These order-of-magnitude agreements are encouraging in light of the scale differences (small-scale experiment v.s. field or large-scale experiment) and the different wave conditions (breaking wave overwash of dunes v.s. unbroken waves on essentially horizontal bottoms.). Figs. 11 and 12 also reveal the difficulty in predicting the relatively small variation of  $C_s$ .

The formula (4) with  $A \approx 0.1$  together with  $\overline{u_* u_*} / Q_* \approx 8$  in Fig.9 may be simplified as

$$C_s = Bw_* \tag{6}$$

where  $B$  = empirical parameter on the order of 0.8. Furthermore, the formula (5) with  $a \approx 5$  and  $f \approx 0.01$  along with  $\overline{u_*^3} / Q_* \approx 4$  in Fig. 10 may simply be rewritten as

$$C_s = bd_* \tag{7}$$

where  $b$  = empirical parameter on the order of 0.02.

For the seven tests consisting of 72 runs listed in Table 1,  $d = 0.38$  mm,  $w = 5.29$  cm/s,  $s = 2.66$  and  $H_s \approx 12$  cm. As a result,  $w_* \approx 0.03$  and  $d_* \approx 1.33$  for this experiment. For the narrow range of the measured values of  $C_s$  for the 72 runs,  $B = 0.63 - 2.22$  with its mean being 0.8 and  $b = 0.014 - 0.049$  with its mean being 0.025. The formulas (6) and (7) are no better than the linear regression between  $Q_s$  and  $Q$  shown in Fig.2 since  $w_*$  is essentially constant and  $d_*$  is constant in this experiment. However, (6) and (7) may be applied to estimate  $C_s$  for other sands.

The variation of the overwash sand concentration  $C_s$  with respect to its median diameter  $d$  estimated using (6) with  $B = 0.8$  as well as (7) with  $b = 0.025$  are shown in Figs. 13 and 14, respectively, where the specific gravity of the sand is assumed to be  $s = 2.6$  and its fall velocity  $w$  is taken to be equal to that of the spherical particle falling in quiet water whose kinematic viscosity is  $\nu = 0.01 \text{ cm}^2/\text{s}$ . In Fig.13, use is made of  $H_s = 0.1, 1$  and  $5$  m because  $w_*$

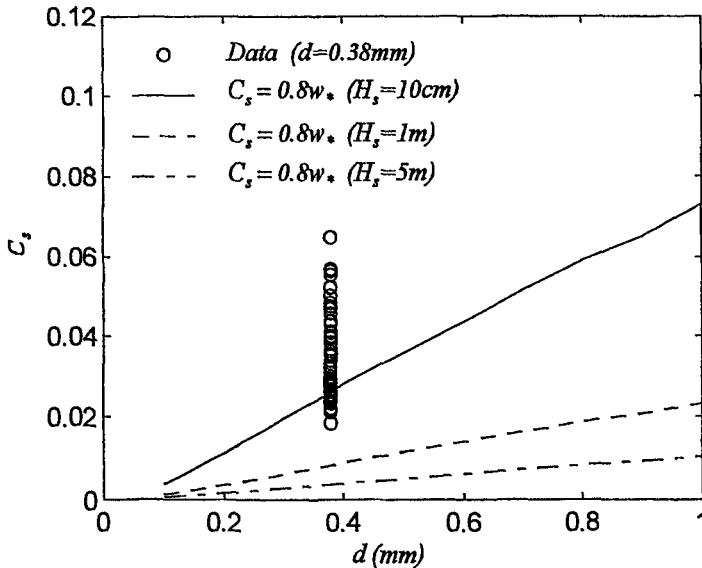


Figure 13: Variation of Sand Concentration  $C_s$  with Median Diameter  $d$  Estimated by  $C_s = 0.8w_*$ .

defined in (4) depends on the incident significant wave height  $H_s$ . Contrary to our expectation, Fig. 13 suggests the increase of  $C_s$  as  $d$  is increased and  $H_s$  is decreased. This indicates the limitation of the formula (2) proposed by Trowbridge and Young (1989) who stated that their formula might be limited to quartz sand whose diameter should not be too different from 0.2 mm. On the other hand, Fig. 14 indicates the increase of  $C_s$  with the decrease of  $d$  as expected. The formula (3) proposed by Ribberink and Al-Salem (1994) was compared with the data with  $d = 0.2 - 1.8$  mm. The rapid increase of  $C_s$  with the decrease of  $d$  in the range  $d < 0.2$  mm in Fig. 14 appears to be unrealistic in view of the physical upper limit of  $C_s \simeq 0.6$ . The range of  $C_s = 0.018 - 0.065$  for the 72 runs in comparison to the variation of  $C_s = 0.025d_s$  for  $d = 0.2 - 1.0$  mm in Fig. 14 implies that it will be difficult to detect the effect of  $d$  on  $C_s$  unless very fine or coarse sands are employed in experiments.

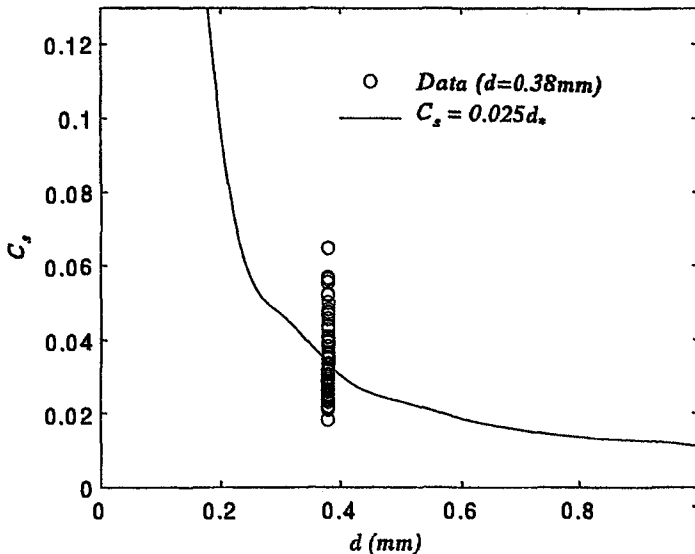


Figure 14: Variation of Sand Concentration  $C_s$  with Median Diameter  $d$  Estimated by  $C_s = 0.025d_s$

## Conclusion

This small-scale experiment on wave overwash of subaerial sand dunes indicates that the net cross-shore sediment transport rate  $q_s$  varies approximately linearly from  $q_s = q_{s2}$  somewhat below SWL, to  $q_s = q_{s1}$  at the dune crest which is approximately the same as the overwash rate  $Q_s$  measured at a short distance landward of the dune crest. The transport rate  $q_{s2}$  is affected by the overtopping rate  $Q$  and may not be assumed to be the same as that for the case of no overtopping. The overwash rate  $Q_s$  may be estimated using the simple relationship of  $Q_s = C_s Q$  with  $C_s \simeq 0.04$  for the median sand diameter  $d = 0.38$  mm but the accuracy of this relationship is limited mostly by the accuracy of the empirical formula for  $Q$  which predicts only the order of magnitude of  $Q$ . In order to extrapolated these small-scale experimental results, the numerical model RBREAK2 for

the overtopping flow is combined with two empirical formulas for  $C_s$ . The computed results suggest that  $C_s$  is on the order of 0.04 except for very fine or coarse sands. This finding is useful for future experiments.

## Acknowledgements

This study is funded by the U.S. Army Research Office, University Research Initiative under Contract No. DAAL03-92-G-0116.

## References

- Hancock, M.W. and Kobayashi, N. (1994). "Wave overtopping and sediment transport over dunes." *Proc. 24th Coast. Engrg. Conf.*, ASCE, 2, 2028-2042.
- Holland, K.T., Holman, R.A. and Sallenger, A.H., Jr. (1991). "Estimation of overwash bore velocities using video techniques." *Coastal Sediments '91*, ASCE, 489-497.
- Kobayashi, N. and Poff, M.T. (1994). "Numerical model RBREAK2 for random waves on impermeable coastal structures and beaches." *Res. Rept. CACR-94-12*, Ctr. for Applied Coast. Res., Univ. of Delaware, Newark, Del.
- Kobayashi, N. and Raichle, A.W. (1994). "Irregular wave overtopping of revetments in surf zones." *J. Wtrway. Port, Coast. Oc. Engrg.*, ASCE, 120(1), 56-73.
- Kobayashi, N., Tega, Y. and Hancock, M.W. (1996). "Wave reflection and overwash of dunes." *J. Wtrway. Port, Coast. Oc. Engrg.*, ASCE, 122(3), 150-153.
- Ribberink, J.S. and Al-Salem, A.A. (1994). "Sediment transport in oscillatory boundary layers in cases of rippled beds and sheet flow." *J. Geophys. Res.*, 99(C6), 12707-12727.
- Steezel, H.J. and Visser, P.J. (1992) "Profile development of dunes due to overflow." *Proc. 23rd Coast. Engrg. Conf.*, ASCE, 3, 2669-2769.
- Trowbridge, J. and Young, D. (1989). "Sand transport by unbroken water waves under sheet flow conditions." *J. Geophys. Res.*, 94(C8), 10971-10991.
- Van der Meer, J.W. and Janssen, J.P.F.M. (1995). "Wave run-up and wave overtopping at dikes." *Wave forces on inclined and vertical wall structures*, ASCE, New York, NY, 1- 27.